Volume 23
Number 5
7 February 2021
Pages 1061–1322

CrystEngComm

rsc.li/crystengcomm

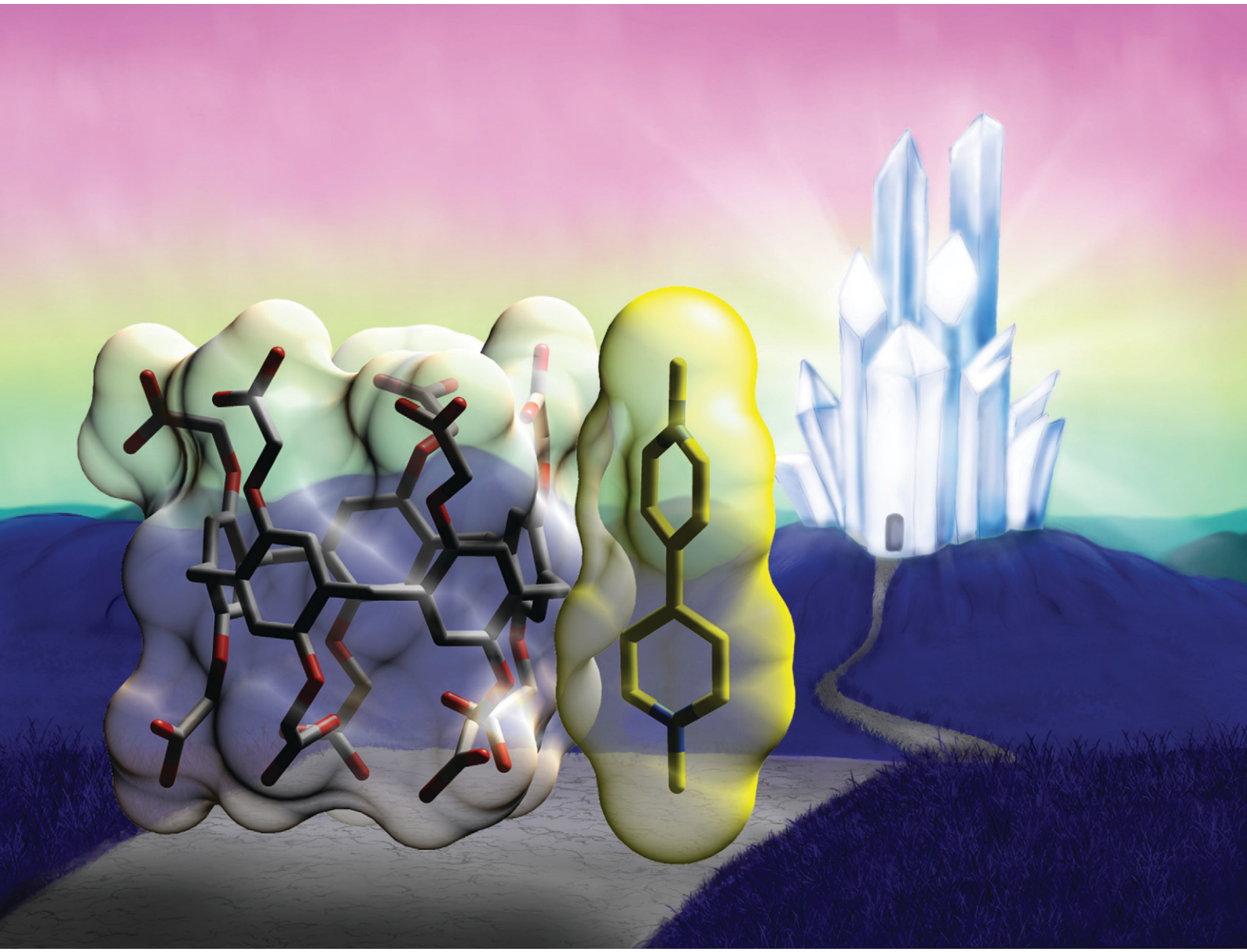

ISSN 1466-8033

ROYAL SOCIETY OF CHEMISTRY

PAPER
Oksana Danylyuk *et al.*
Unveiling the structural features of the host–guest complexes of carboxylated pillar[5]arene with viologen derivatives

CrystEngComm

ROYAL SOCIETY OF CHEMISTRY

PAPER

View Article Online
View Journal | View Issue

Cite this: *CrystEngComm*, 2021, **23**, 1075

Unveiling the structural features of the host–guest complexes of carboxylated pillar[5]arene with viologen derivatives†

Helena Butkiewicz, Sandra Kosiorek, Volodymyr Sashuk and Oksana Danylyuk *

Despite the impressive progress in the study of the aqueous host–guest chemistry of carboxylated pillar[*n*]arenes, these macrocyclic molecules represent a completely unexplored class of molecular building blocks in the solid state supramolecular chemistry. Here we describe the formation of crystalline host–guest complexes of carboxylated pillar[5]arene with four viologen derivatives, emphasizing its inclusion and self-assembly behavior in the presence of cationic electron-deficient guests. The macrocyclic cavity is prone to slight distortion upon the inclusion of alkyl viologens, but competitive inclusion of ethanol molecules takes place in the case of bulky benzyl viologen. The different distribution of carboxylic *versus* carboxylate substituents of pillar[5]arene renders self-assembly *via* carboxylic–carboxylic or carboxylic–carboxylate supramolecular synthons.

Received 29th October 2020,
Accepted 9th December 2020

DOI: 10.1039/d0ce01579b

rsc.li/crystengcomm

Introduction

The supramolecular chemistry of the water-soluble carboxylated pillar[*n*]arenes (**CPA*n***) has been flourishing since their discovery by Ogoshi in 2010.[1] The unique intrinsically rigid and highly symmetric macrocyclic structure decorated with carboxyl groups provides them with outstanding host–guest binding properties in aqueous media.[2] The **CPA*n*** appear to be relatively non-toxic[3] and of tremendous potential application in drug delivery,[4] as antitumor agents,[5] and supramolecular catalysts[6] due to their excellent ability to complex various guest molecules. Despite the impressive progress in the study of their aqueous host–guest and self-assembly properties, these macrocyclic molecules represent a completely unexplored class of molecular building blocks in the solid state supramolecular and coordination chemistry. This is very surprising considering (i) the combination of a rigid electron-rich cavity and flexible carboxylic linkers making them highly promising candidates for the design of solid-state assemblies of various topologies; (ii) the presence of multiple carboxylic groups that can be completely or partially deprotonated, potentially inducing rich binding modes and interesting structures of high dimensionality; (iii) they can act both as multiple hydrogen bond donors and acceptors depending on the degree of deprotonation; (iv) the well-established supramolecular synthons may be used to drive the self-assembly with carboxylic acids. These characteristics may lead to the discovery of the novel class of crystalline materials constructed from the cavity containing macrocyclic building blocks.[7]

Considering these aspects, we recently began investigating their solid-state supramolecular chemistry and reported the first structural authentication of carboxylic acid substituted pillar[5]arene (**CPA5**), its basic self-assembly properties and formation of a host–guest complex with active pharmaceutical ingredient tetracaine.[8] Our current work is focused on the utilization of **CPA5** as a building block in the supramolecular architectures through: 1) exploitation of the properties of its macrocyclic cavity towards guest inclusion, 2) study of the solid-state assembly of **CPA5** *via* carboxylic–carboxylic and carboxylic–carboxylate supramolecular synthons. Here we show the formation of host–guest complexes of **CPA5** with four viologen derivatives,

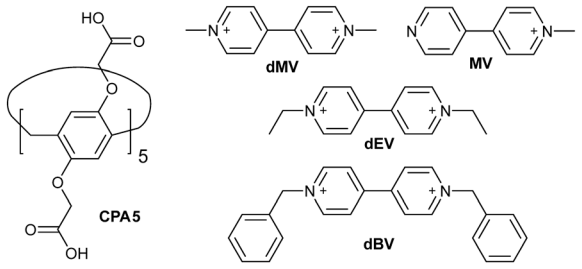

Fig. 1 Chemical structure of carboxylated pillar[5]arene and four viologen guests used in the host–guest study.

Institute of Physical Chemistry, Polish Academy of Sciences, Kasprzaka 44/52, 01-224 Warsaw, Poland. E-mail: odanylyuk@ichf.edu.pl

† Electronic supplementary information (ESI) available: X-ray crystallographic files in CIF format. CCDC 2040336–2040339. For crystallographic data in CIF or other electronic format see DOI: 10.1039/d0ce01579b

emphasizing the inclusion and self-assembly behavior of **CPA5** with cationic guests in the solid state, Fig. 1. Viologens are commonly used in the supramolecular chemistry to fabricate capsular or threaded host–guest assemblies both in solution and solid state.[9] Their cationic electron-deficient nature makes them perfect guests for electron-rich and/or anionic host molecules. Notably, the dimethyl viologen salt (paraquat) was the first guest to reveal the inclusion properties of deca-anionic form of **CPA5** in an aqueous solution.[1] The molecular recognition of paraquat by larger homologue **CPA6** in water has been proposed as a supramolecular treatment of paraquat poisoning.[10] It should be emphasized that no crystal structure of a fully anionic form of **CPA5** has been reported so far, despite the impressive progress in its solution studies and excellent solubility in water. On the contrary, fully carboxylic functionality of **CPA5** renders its low solubility in aqueous solutions, and only the addition of cosolvent (ethanol) as found by us[8] entails a significant increase of the solubility of the carboxylic form of **CPA5** enabling both solution studies and crystallization of its complexes. The possibility to tune the solubility of **CPA5** not only by pH, but by the addition of cosolvent opens up new opportunities in the **CPA5** aqueous chemistry. One direction is to integrate the **CPA5** macrocycle as a basic supramolecular building block in the crystal engineering using well-studied supramolecular synthons involving carboxylic acid groups.

Results and discussion

Cocrystallization of dimethyl viologen (*N*,*N*′-dimethyl-4,4′-bipyridinium) dichloride, also known as paraquat, with **CPA5** from the water–ethanol solution afforded prismatic crystals of the host–guest complex **I**. The orange color of the crystalline complex was notably different from the solid forms of both host **CPA5** and guest dimethyl viologen (**dMV**) components (white powders). X-ray single crystal analysis revealed a 1 : 1 host–guest inclusion complex of the composition [**dMV@CPA5**]·5.27(H_2O) in the $P2_1/c$ space group of the monoclinic system. The asymmetric unit comprises one **CPA5** molecule, one paraquat cation (modelled as disordered over two positions) included into the host cavity, and water molecules. The dicationic nature of the guest suggests the deprotonation of two of the ten carboxylic substituents of the macrocyclic host to satisfy the electroneutrality of the complex. The **dMV** penetrates the pentagonal cavity of **CPA5** in an asymmetric way with one of the methylpyridinium moieties being encircled by aromatic walls of the macrocycle, while the second methylpyridinium unit is embraced by aliphatic arms of the 'entrance rim', Fig. 2a. The depth of the inclusion measured as the distance between the mean plane determined by five methylene carbon atoms of the **CPA5** macrocyclic core and centroid of the C–C bond between two pyridinium rings of the **dMV** is equal to 3.4 Å (3.8 Å for the second position of **dMV**). The crystals have an orange color suggesting a π–π charge-transfer of the donor–acceptor type between electron-rich aromatic walls of **CPA5** and electron-poor pyridinium rings of the **dMV** guest. One of the phenyl rings of the **CPA5** is indeed approximately parallel to the included pyridinium ring of the guest (7° tilt between the mean planes), and the closest donor–acceptor distance is at 3.24 Å (between C3D and C5X). Besides hydrophobic effect, electrostatic attraction and charge transfer, the host–guest complex is stabilized by the C–H···π hydrogen bonding between the included pyridinium ring of the **dMV** and aromatic walls of **CPA5** (Fig. 2b); the shortest C···π (centroid) distances are 3.21 and 3.16 Å. The second methylpyridinium moiety that protrudes from the cavity is involved in the C–H···π and C–H···O interactions with the host.

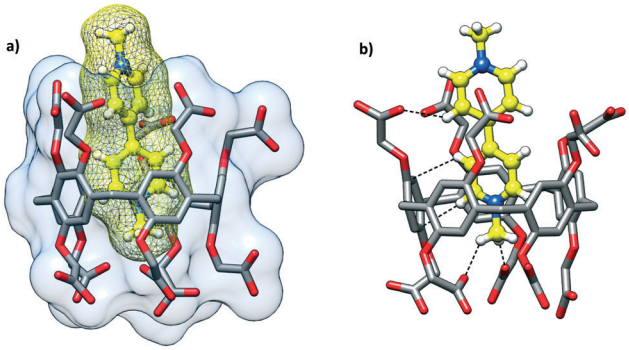

Fig. 2 The host–guest complex **I** of **CPA5** with dimethyl viologen **dMV** (paraquat) highlighting the (a) inclusion mode and (b) C–H···π and C–H···O interactions between the guest and cavity interior.

While the shape of the **CPA5** macrocyclic core resembles a regular pentagon, the closer look reveals some deviation from regular Euclidean geometry. For a regular pentagon, the interior angles are 108°, while the sp^3 hybridization of the bridging methylene groups in pillar[5]arene would favor the bonding angle of 109.28°. The structural strain within the macrocycle is manifested in the expansion of the valence angles of CH_2 bridges to ~111° from the theoretical sp^3 value and slight bending and/or tilting of aromatic walls from the

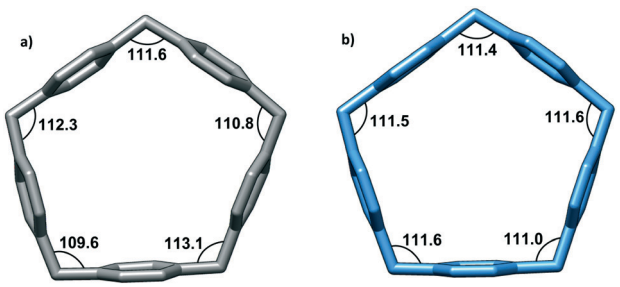

Fig. 3 The geometry of the **CPA5** pentagonal cavity in the host–guest inclusion complexes with (a) dimethyl viologen **dMV** (paraquat) and (b) ethanol.[8] Note the wider range of methylene bonding angles in the **dMV@CPA5** complex (109.6–113.1°) than in the **EtOH@CPA5** complex (111.0–111.6°), evidencing a more pronounced distortion of the macrocycle from a regular Euclidean pentagon upon inclusion of bulky guest **dMV**.

center of the cavity as shown from the crystal structure of the carboxylic acid substituted pillar[5]arene, in which the macrocyclic cavity is taken by two ethanol molecules (refcode KOVPES), Fig. 3b.[8] Moreover, the inclusion of the bulky paraquat into the **CPA5** cavity causes even further distortion of the macrocycle from a regular Euclidean pentagon, Fig. 3a.

Ten carboxylic/carboxylate groups of **CPA5** are involved in extensive O–H···O hydrogen bonding (HB) with adjacent **CPA5** (Fig. 4) and multiple water molecules in the crystal lattice. Surprisingly, the distance range of the O–H···O HB between adjacent **CPA5** molecules of 2.45–2.60 Å suggests a very strong HB, which is not observed for the previously reported **CPA5** inclusion complex with ethanol in which all of the carboxylic functions of the macrocycle are protonated.[8] Moreover, there are no carboxylic–carboxylic cyclic dimers typical for the self-assembly of fully protonated **CPA5**, suggesting strong preference of carboxylic···carboxylate single HB assembly of **CPA5** comprising both anionic and neutral carboxylic functionalities. The shortest HB of 2.446(4) Å is a single HB realized between carboxylic and carboxylate groups related by an inversion center, O5D–(1/2 H5D1)···(1/2 H5D1)^3–O5D^3, [symmetry code: (3) $-x + 1, -y + 1, -z$]. The 50% occupancy of the H5D1 atom was imposed as a consequence of the formation of the hydrogen bonded carboxylic–carboxylate linear dimer over an inversion center. Besides obvious disorder of the position of the hydrogen atom, there is also a crystallographically imposed disorder of carboxylic and carboxylate groups over an inversion center, which was not accounted during refinement due to their similar geometry. This type of disorder was assumed based on statistical data extracted from the CSD on the distance distribution between two O atoms involved in the intermolecular HB for carboxylic–carboxylic and carboxylic–carboxylate dimer structures with low *R*-factors ($R \leq 0.05$).[11] The average hydrogen-bonded distance between two O atoms in carboxylic–carboxylate dimers is very short (2.54 ± 0.06 Å). Otherwise, the average distance distribution between two O atoms in the single carboxylic–carboxylic HB dimers is 2.66 ± 0.05 Å. Surprisingly, the shortest HB distances between two O atoms of carboxylic–carboxylate dimers responsible for the self-assembly of adjacent **CPA5** of 2.446(4) and 2.469(3) Å (O3A–H3A···O3D) are even shorter than the average distance distribution for carboxylic–carboxylate synthons in the CSD. Such very short hydrogen bonds in the carboxylic–carboxylate dimers are rather typical for the intramolecular HB in the mono-anions of dicarboxylic acids (oxalic, malonic, and maleic) and phthalic acid; the average distance distribution is 2.43 ± 0.04 Å.[11]

The short donor–acceptor distances are a characteristic for short strong hydrogen bonds (less than 2.5 Å for the O–H···O HB).[12] These interactions are believed to be partly covalent in nature based on various experimental and theoretical techniques, such as infrared and NMR spectroscopies, X-ray and neutron diffraction.[13] The potential energy surface of very short HBs approach the shape of symmetric single-well potential with a reduced barrier for proton migration rather than the double-well potential of the typical HB.[14] Since the **CPA5** solid state supramolecular chemistry is still in the flower bud, it is difficult to say if an unusually short carboxylic–carboxylate HB is typical and dominant for the assembly of **CPA5** with mixed anionic and neutral carboxylic functionalities. Obviously, it would depend on the presence of competitive alternative HB motifs, for example the pyridyl nitrogen as a HB acceptor, and the number of deprotonated *versus* neutral carboxylic groups. Besides the short carboxylic–carboxylate HB guiding the assembly, we noted several carboxylic–water HBs and the absence of the carboxylic–carboxylic HB. The feature of the assembly of **CPA5** with mixed anionic and neutral carboxylic functionalities is the network of carboxylic–carboxylate HB **CPA5** in contrast to the chain-like assembly of the neutral form of **CPA5** guided by the cyclic carboxylic–carboxylic HB supramolecular synthons.[8]

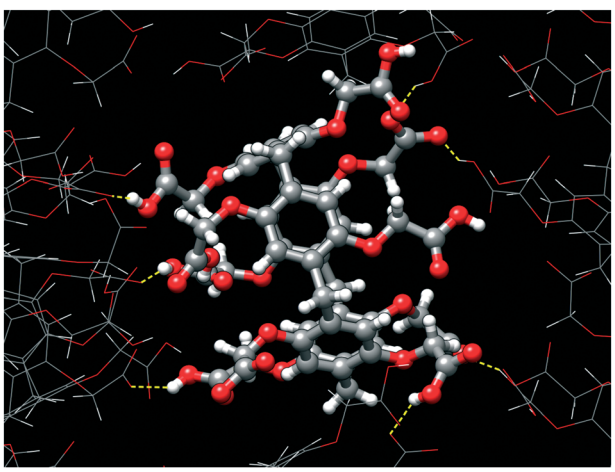

Fig. 4 The hydrogen bonds generated by the **CPA5** molecule with adjacent **CPA5** in the crystal lattice of **dMV@CPA5**. The distance range of O–H···O of 2.45–2.60 Å suggests a very strong hydrogen bonding characteristic for a charge-assisted carboxylic–carboxylate synthon. Note the absence of carboxylic–carboxylic association.

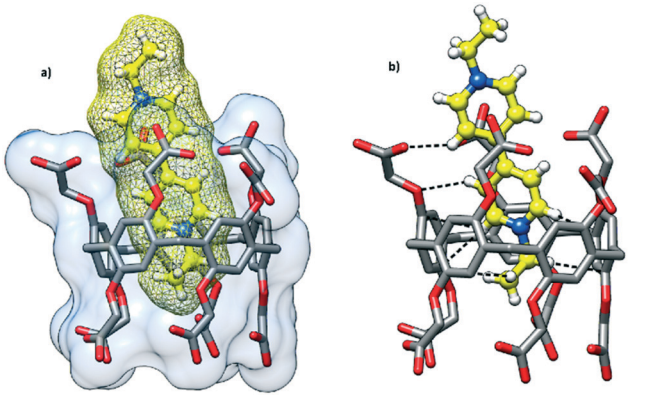

Fig. 5 Host–guest complex **II** of **CPA5** with diethyl viologen **dEV** highlighting the (a) inclusion mode and (b) C–H···π and C–H···O interactions between the guest and cavity interior.

The cocrystallization of ethyl viologen (*N*,*N*′-diethyl-4,4′-bipyridinium)dibromide (**dEV**) with **CPA5** from the water–ethanol solution afforded yellow prismatic crystals of host–guest complex **II**. X-ray single crystal analysis revealed a 1 : 1 host–guest inclusion complex of the composition [**dEV@CPA5**]·6.5H_2O in the $P2_1/n$ space group of the monoclinic system, Fig. 5a. The asymmetric unit comprises one **CPA5** molecule, one ethyl viologen dication included into the host cavity, and water molecules. The complex is similar to the previously described **dMV@CPA5**, however, there are some notable differences. The inclusion of the bipyridinium core of the guest is shallower than that in the **dMV@CPA5** complex; the depth of the inclusion is 4.1 Å, comparable to 3.4 and 3.8 Å (two disordered positions of **dMV**) in the **dMV@CPA5** complex. The ethylpyridinium moiety immersed in the cavity is held *via* C–H···π interactions; the shortest C···π (centroid) distance is at 3.31 Å, Fig. 5b. The closest donor–acceptor distance is at 3.23 Å (C3C···C5P) involving edge-to-edge orientation of the donor (**CPA5**) and acceptor (included pyridinium moiety) π systems responsible for the yellow color of the host–guest crystals. The second ethylpyridinium moiety protrudes from the cavity interacting *via* the C–H···O hydrogen bonding with the carboxyl groups of host **CPA5** and adjacent **CPA5** in the crystal lattice. The distortion of the **CPA5** pentagonal cavity from a regular pentagon due to the inclusion of **dEV** is similar to the case of **dMV@CPA5** host–guest complex **I**.

The self-assembly of adjacent **CPA5** macrocycles is featured by realization of both carboxylic–carboxylate and carboxylic–carboxylic types of HB, Fig. 6. The two short distances between pairs of carboxyl partners involved in the intermolecular HB are 2.475(5) and 2.572(4) Å, evidencing the carboxylic–carboxylate synthon. The two long distances of 2.649(4) and 2.669(4) Å are typical for carboxylic–carboxylic dimers. These carboxylic–carboxylic dimers involve a single HB linking the two units. No cyclic carboxylic–carboxylic dimers have been identified in the **dEV@CPA5** assembly. **CPA5** are also involved in the extensive carboxylic–water HB.

The cocrystallization of **CPA5** with 1-methyl-4,4′-bipyridinium (**MV**) iodide resulted in yellow prismatic crystals of host–guest complex **III**. The asymmetric unit comprises one **CPA5**, one guest **MV** included into the host macrocyclic cavity, one magnesium cation coordinated to **CPA5**, and 11.5 water molecules, Fig. 7. The presence of a magnesium cation as a component of the host–guest crystalline complex was rather unexpected, as the magnesium chloride has been used by us as an additive in all crystallization experiments with **CPA5** to produce better quality single crystals. The magnesium ion was not present in the crystal lattice of the **CPA5** complexes with **dMV** and **dEV**. The reason for the simultaneous guest inclusion and coordination of magnesium to **CPA5** carboxyl groups may be related to the monocationic type of guest **MV** instead of dicationic **dMV** and **dEV** without magnesium interference. However, additional structural studies on the coordination mode of magnesium (as well as other metal cations) with **CPA5** and mixed coordination/host–guest complexes are necessary to give more insight into the problem. No crystal structure on the coordination complexes of **CPA5** has been reported so far, which is surprising considering the tremendous interest in the incorporation of **CPA*n***'s into metal–organic frameworks, for example, for drug loading and release.[15] The crystal structure was solved and refined in monoclinic space group *I*2/*a*. The methylpyridinium moiety of the guest penetrates the central cavity of the host in a manner similar to **dMV@CPA5**, while the pyridine part of the guest is embraced by aliphatic substituents of the 'entrance' rim with pyridine nitrogen protruding from the host rim. The depth of the inclusion is 3.7 Å. The main difference between monocationic guest **MV** and dicationic **dMV** besides charge is the presence of pyridine nitrogen in the **MV** guest; the excellent acceptor of HB was realized in the carboxylic acid–

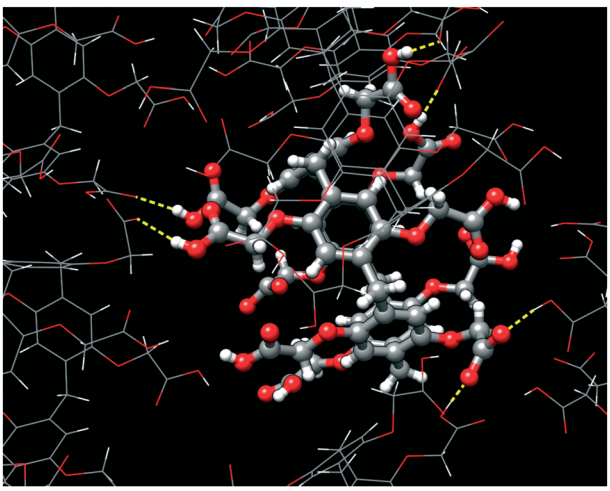

Fig. 6 The hydrogen bonds generated by a **CPA5** molecule with adjacent **CPA5** in the crystal lattice of **dEV@CPA5**. The distance range of O–H···O of 2.47–2.67 Å suggests the realization of both carboxylic–carboxylate and carboxylic–carboxylic supramolecular synthons.

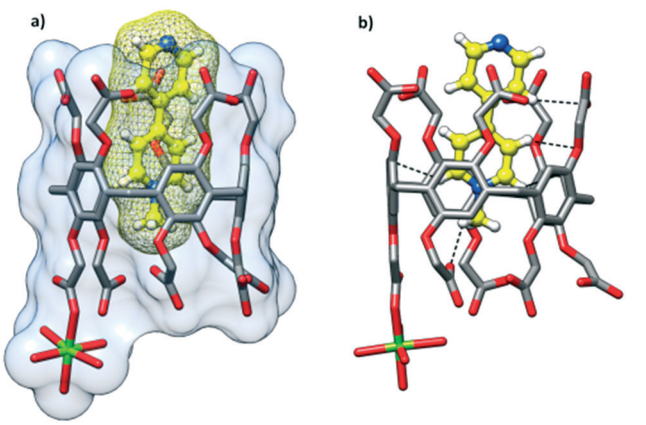

Fig. 7 Host–guest complex **III** of **CPA5** with methyl viologen **MV** highlighting the (a) inclusion mode of **MV** and coordination mode of magnesium cation (in green); (b) C–H···π and C–H···O interactions between the guest and cavity interior.

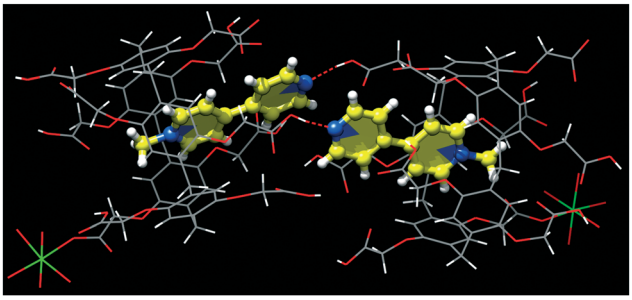

Fig. 8 The hydrogen bonding between carboxylic group of **CPA5** and N-pyridine nitrogen of the guest from symmetry-equivalent **MV@CPA5**.

pyridine heterosynthon.[16] Thus, we expected the competitive participation of **MV** as an acceptor in the HB network between adjacent **CPA5** hosts. Indeed, single crystal X-ray analysis has shown that the pyridine nitrogen of the included guest act as the acceptor of HB from one of the carboxylic groups of the symmetry-equivalent **CPA5** (O–H···N distance 2.591 Å) altering exclusive O–H···O HB assembly observed in the **dMV@CPA5** and **dEV@CPA5** complexes, Fig. 8.

Magnesium cation is coordinated directly to three carboxyl groups (two carboxylate and one carboxylic) of three adjacent **CPA5** in the monodentate mode, in other words, three of the ten carboxyl substituents of each **CPA5** are coordinated to magnesium ions (Mg–O distances are in the range of 2.00–2.15 Å). Interestingly, the coordination is realized only on one of the rims of **CPA5** – the 'free' rim opposite to the 'entrance' rim occupied with the pyridine moiety of the guest. The magnesium cation is in the typical octahedral coordination with three aqua ligands complementing the coordination sphere in addition to three carboxyl oxygen atoms of **CPA5**, Fig. 9a. Monodentately bound carboxylates stabilize themselves further *via* HB in the first coordination sphere between one carboxylic ligand (donor) and one carboxylate ligand (HB acceptor) (2.509 Å), and between one aqua ligand (HB donor) and one carboxylate (2.679 Å). There is also additional HB to second-sphere functionalities. Such coordination mode leads to the 1-D coordination polymer consisting of double-strand of **CPA5**, Fig. 9b. Besides coordination through an Mg cation, adjacent **CPA5** are assembled *via* O–H···O HB; two short distances between oxygen atoms of 2.480 and 2.509 Å imply carboxylic–carboxylate association; one long distance 2.724 Å corresponds to the carboxylic–carboxylic supramolecular synthon.

The cocrystallization of **CPA5** with benzyl viologen (*N*,*N*′-dibenzyl-4,4′-bipyridinium) (**dBV**) chloride resulted in red plate-like crystals of host–guest complex **IV**. X-ray single crystal analysis revealed a host–guest complex of the exclusion type of 2 : 1 stoichiometry in the $P\bar{1}$ space group. The asymmetric unit comprises one **CPA5** molecule, two ethanol molecules occupying the host cavity, half of the benzyl viologen **dBV** dication lying on the inversion center outside of the host cavity, (Fig. 10) and water molecules. The

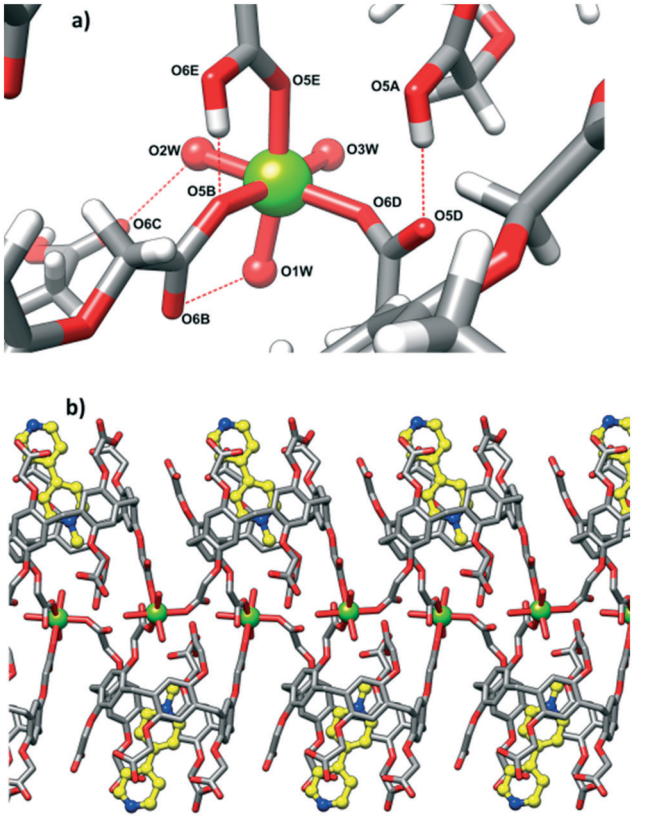

Fig. 9 (a) The coordination environment of a magnesium cation in complex **III**. Two carboxylate, one carboxylic and three aqua ligands constitute the octahedral coordination of Mg^{2+}. Such coordination mode is stabilized by additional hydrogen bonding in the first coordination sphere between carboxylic and carboxylate ligands (O–H O distance of 2.509 Å) and between water and carboxylate (O–H O distance of 2.679 Å). (b) The 1-D double-strand coordination polymer is formed by the coordination of Mg^{2+} to three **CPA5** molecules.

crystal structure is characterized by a high degree of disorder; eight of the ten carboxyl substituents of **CPA5**, ethanol molecules inside the cavity, benzyl viologen dication and water molecules were modeled as disordered. Nevertheless, the quality of the structure and appropriate modeling of

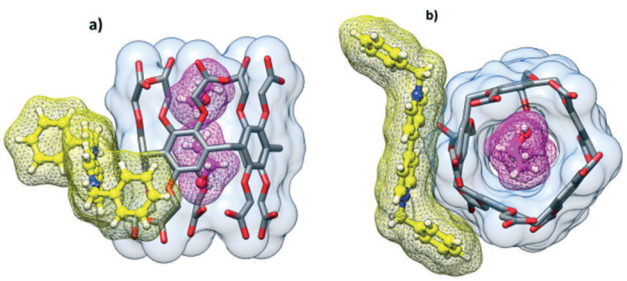

Fig. 10 Host–guest complex **IV** of **CPA5** with dibenzyl viologen **dBV**. The macrocyclic cavity is occupied by two ethanol molecules (in magenta), while dibenzyl viologen (in yellow) is complexed outside the cavity: (a) side view and (b) top view of the complex. The asymmetric unit contains only half of the **dBV** dication lying on the inversion center; the entire **dBV** is shown here for the appropriate illustration of the host–guest chemistry.

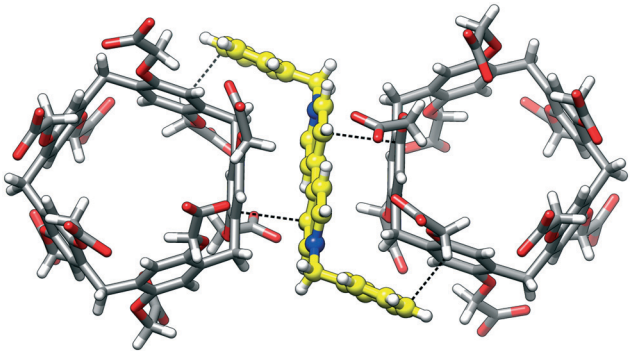

Fig. 11 The sandwiching of dibenzyl viologen **dBV** between outer walls of two **CPA5** molecules in complex **IV** explaining the deep red color of crystals typical for the charge-transfer of the donor–acceptor type. The electron-deficient viologen moiety of the guest is almost parallel to electron-rich aromatic walls of **CPA5** (6° tilt between the mean planes); the closest donor–acceptor distance is at 3.29 Å (shown as dashed black line between viologen and aromatic carbons of **CPA5**). The complexation mode is also stabilized by C–H···π host–guest interactions.

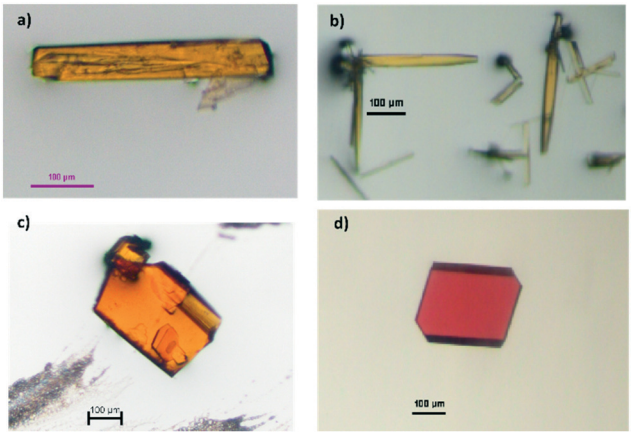

Fig. 13 Optical microscopy images of the host–guest crystals of **CPA5** with dimethyl viologen (a), diethyl viologen (b), methyl viologen (c) and dibenzyl viologen (d). The charge transfer of the donor–acceptor type between electron-rich **CPA5** cavity and electron-poor viologen guests is responsible for the crystal colour. Note that the intense red colour is a characteristic for the sandwiching of the dibenzyl viologen guest between exo-walls of two **CPA5** molecules.

disorder were sufficient to recognize the host–guest chemistry and assembly mode of the complex in the solid state. The macrocyclic cavity is filled with two ethanol molecules as in **EtOH@CPA5** which was reported by us previously.[8] Obviously, the inclusion of the bulky **dBV** would require the significant distortion of the **CPA5** cavity and thus was energetically unfavorable.

Despite the lack of the inclusion complexation between **dBV** and **CPA5**, the deep red color of crystals suggests charge transfer between the electron-rich walls of **CPA5** and electron-poor viologen moiety. Indeed, close inspection of the surroundings of **dBV** in the crystal lattice revealed its sandwiching between outer walls of two **CPA5** macrocycles, Fig. 11. The aromatic walls of **CPA5** are approximately parallel to the inserted viologen core of the **dBV** (6° tilt between mean planes); the closest donor–acceptor distance is at 3.29 Å (C3A···C4X). The 2 : 1 stoichiometry between **CPA5** and dicationic **dBV** implies that only one of the ten carboxyl substituents of **CPA5** is in the anionic carboxylate form. The self-assembly mode of adjacent **CPA5** also resembles that of **EtOH@CPA5** in a fully carboxylic form, Fig. 12.[8] The only two ordered carboxylic groups are engaged in the HB cyclic dimer with O–H···O distances of 2.622 and 2.667 Å. The conformation of **CPA5** resembles a regular pentagon as in the **EtOH@CPA5** complex in contrast to inclusion complexes **dMV@CPA5** and **dEV@CPA5** with distorted cavities.

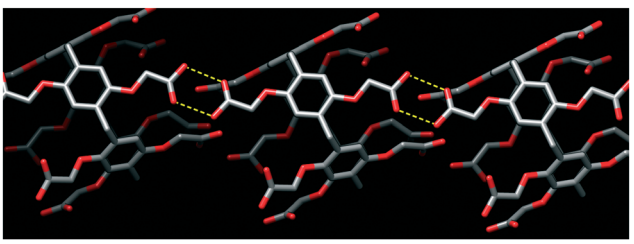

Fig. 12 The self-assembly between adjacent **CPA5** *via* the carboxylic–carboxylic cyclic supramolecular synthon in host–guest complex **IV** of **CPA5** with dibenzyl viologen. The identification of other hydrogen bonding types was not attempted due to the heavy disorder of eight of the ten carboxylic substituents of the **CPA5** (only one position for each of the disordered groups is depicted).

Conclusions

CPA5 have been shown to be a versatile building block for the host–guest assemblies with viologen derivatives both of inclusion and exclusion types. In all complexes, the charge-transfer between the electron-rich macrocyclic cavity and electron-deficient viologen moiety of the guest contributed to the complexation, Fig. 13. The different distribution of carboxylic *versus* carboxylate substituents of **CPA5** renders self-assembly *via* carboxylic–carboxylic or carboxylic–carboxylate supramolecular synthons. It appears from the studied complexes that very short HB with O–H···O distances less than 2.50 Å are typical for the self-assembly of **CPA5** with mixed carboxylic and carboxylate functionalities. Further studies will deal with the possibility to disrupt these preferable types of **CPA5** association through targeted heterosynthon formation (for example carboxylic acid–pyridine) by the introduction of multiple or multivalent guest partners. The presence of ten carboxylic/carboxylate functional groups provides both opportunities and challenges in the future design of self-assembled architectures based on the **CPA5** building block. On the one hand, it affords the possibility to participate in various intermolecular interactions in addition to the inherent cavity features, thus there is a strong temptation to utilize multivalent **CPA5** for the supramolecular fabrication of multicomponent crystalline materials. On the other hand, gaining control over multiple/

competing interactions when utilizing **CPA5** might be a challenge for crystal engineers. The design strategies based on the use of bulky organic cations[17] and/or directing metal ions,[18] templating effect of solvent,[19] and outer surface interactions[20] lend some insight into the targeted self-assembly of cavity-containing macrocyclic hosts. These strategies have been demonstrated to be successfully implemented in many examples with water-soluble *p*-sulfonatocalix[*n*]arene[21] and cucurbit[*n*]uril[22] architectures, and may be proved useful in gaining some level of control in constructing **CPA5** complex assemblies. It is clear, however, that much work remains to be done to study the self-assembly and crystallization of **CPA5** complexes and, in particular, to reveal and understand the host–guest and coordination solid-state chemistry of **CPA5**. Our future work will focus on the further utilization of **CPA5** as a building block in the supramolecular architectures while mapping out their assembly properties in the solid-sate.

Experimental

Materials

Dimethyl, methyl, diethyl and dibenzyl viologens were purchased from Sigma-Aldrich. Carboxylic acid substituted pillar[5]arene was synthesized according to a literature procedure.[23]

Crystallization conditions

Complex I. 1 mg of **CPA5** and 8.5 mg of $MgCl_2$ were dissolved in 1.5 ml of a 1 : 1 water–ethanol mixture under gentle heating. The solution of 0.8 mg of dimethyl viologen (1,1′-dimethyl-4,4′-bipyridinium) dichloride, also known as paraquat, in 1 ml of a 1 : 1 water–ethanol mixture was slowly added to the solution of **CPA5**. The diffraction-quality crystals of complex **I dMV@CPA5** grew after several days.

Complex II. 0.9 mg of **CPA5** and 4.8 mg of $MgCl_2$ were dissolved in 1.5 ml of a 1 : 1 water–ethanol mixture under gentle heating. The solution of 0.6 mg of diethyl viologen (1,1′-diethyl-4,4′-bipyridinium) dibromide in 0.5 ml of a 1 : 1 water–ethanol mixture was slowly added to the solution of **CPA5**. The diffraction-quality crystals of complex **II dEV@CPA5** grew after several days.

Complex III. 1 mg of **CPA5** and 8.7 mg of $MgCl_2$ were dissolved in 1.5 ml of a 1 : 1 water–ethanol mixture under gentle heating. The solution of 1.1 mg of methyl viologen (1-methyl-4,4′-bipyridinium) iodide in 0.5 ml of a 1 : 1 water–ethanol mixture was slowly added to the solution of **CPA5**. The diffraction-quality crystals of complex **III MV**@Mg(**CPA5**) grew after several days.

Complex IV. 1.2 mg of **CPA5** and 7.2 mg of $MgCl_2$ were dissolved in 1.5 ml of a 1 : 1 water–ethanol mixture under gentle heating. The solution of 0.5 mg of dibenzyl viologen (1,1′-dibenzyl-4,4′-bipyridinium) dichloride in 0.5 ml of a 1 : 1 water–ethanol mixture was slowly added to the solution of **CPA5**. The diffraction-quality crystals of complex **IV** 2(EtOH)@(**CPA5**)(**dBV**) grew after several days.

Crystallography

The crystals were embedded in the inert perfluoropolyalkylether (viscosity 1800cSt; ABCR GmbH) and mounted using Hampton Research Cryoloops. The crystals were flash cooled to 100.0(1) K in a nitrogen gas stream and kept at this temperature during the experiments. The X-ray data were collected on a SuperNova Agilent diffractometer using CuKα radiation (λ = 1.54184 Å). The data were processed with CrysAlisPro.[24] The structures were solved by direct methods and refined using SHELXL[25] under WinGX.[26] The figures were prepared using Chimera.[27]

Crystal data for I. $(C_{55}H_{48}O_{30})\cdot(C_{12}H_{14}N_2)\cdot 5.27(H_2O)$, Mr = 1470.1, orange blocks, monoclinic, space group $P2_1/c$, a = 21.4549(4), b = 12.5308(1), c = 26.2757(4) Å, β = 111.934(2)°, V = 6552.8(2) Å^3, Z = 4, ρ_{calc} = 1.49 g cm^{-3}, μ(CuKα) = 0.79 mm^{-1}, θ_{max} = 72.11°, 45 391 reflections measured, 12 768 unique, 1159 parameters, R = 0.069 and wR = 0.199 (R = 0.094 and wR = 0.219 for all data). GooF = 1.06. CCDC 2040337.

Crystal data for II. $(C_{55}H_{48}O_{30})\cdot(C_{14}H_{18}N_2)\cdot 6.5(H_2O)$, Mr = 1520.3, yellow blocks, monoclinic, space group $P2_1/n$, a = 21.8515(1), b = 12.3750(6), c = 27.435(2) Å, β = 112.883(9)°, V = 6834.9(9) Å^3, Z = 4, ρ_{calc} = 1.48 g cm^{-3}, μ(CuKα) = 1.04 mm^{-1}, θ_{max} = 67.80°, 43 895 reflections measured, 12 194 unique, 975 parameters, R = 0.072 and wR = 0.180 (R = 0.123 and wR = 0.204 for all data). GooF = 0.88. CCDC 2040338.

Crystal data for III. $[Mg(C_{55}H_{47}O_{30})\cdot 3(H_2O)](C_{11}H_{11}N_2)\cdot 8.5(H_2O)$, Mr = 1590.6, yellow blocks, monoclinic, space group $I2/a$, a = 35.5280(3), b = 12.9487(1), c = 33.1933(3) Å, β = 105.019(1)°, V = 14 748.7(2) Å^3, Z = 8, ρ_{calc} = 1.43 g cm^{-3}, μ(CuKα) = 1.12 mm^{-1}, θ_{max} = 66.60°, 30 850 reflections measured, 12 912 unique, 1064 parameters, R = 0.099 and wR = 0.283 (R = 0.105 and wR = 0.289 for all data). GooF = 0.97. CCDC 2040339.

Crystal data for IV. $(C_{55}H_{49}O_{30})\cdot 0.5(C_{24}H_{22}N_2)\cdot 2(C_2H_5OH)\cdot 3(H_2O)$, Mr = 1505.3, red plates, triclinic, space group $P\bar{1}$, a = 12.9186(5), b = 13.6147(6), c = 21.7390(8) Å, α = 89.925(3), β = 81.101(3), γ = 76.021°, V = 3663.0(3) Å^3, Z = 2, ρ_{calc} = 1.37 g cm^{-3}, μ(CuKα) = 0.94 mm^{-1}, θ_{max} = 69.71°, 29 147 reflections measured, 13 627 unique, 1132 parameters, R = 0.106 and wR = 0.284 (R = 0.120 and wR = 0.297 for all data). GooF = 0.99. CCDC 2040336.

Conflicts of interest

There are no conflicts to declare.

Acknowledgements

The project was funded by the National Science Centre of Poland (grant PRELUDIUM 14 nr 2017/27/N/ST5/01931).

Notes and references

1 T. Ogoshi, M. Hashizume, T. Yamagishi and Y. Nakamoto, *Chem. Commun.*, 2010, **46**, 3708.
2 T. Xiao, W. Zhong, L. Xu, X. Q. Sun, X. Y. Hu and L. Wang, *Org. Biomol. Chem.*, 2019, **17**, 1336; N. Song, T. Kakuta, T.

Yamagishi, Y.-W. Yang and T. Ogoshi, *Chem*, 2018, **4**, 2029; P. J. Cragg, *Isr. J. Chem.*, 2018, **58**, 1194; Y. Liu, F. Zhou, F. Yang and Da Ma, *Org. Biomol. Chem.*, 2019, **17**, 5106; T. Kakuta, T. Yamagishi and T. Ogoshi, *Acc. Chem. Res.*, 2018, **51**, 1656; H. Zhang, Z. Liu and Y. Zhao, *Chem. Soc. Rev.*, 2018, **47**, 5491; S. Dasgupta and P. S. Mukherjee, *Org. Biomol. Chem.*, 2017, **15**, 762; N. L. Strutt, H. Zhang, S. T. Schneebeli and J. F. Stoddart, *Acc. Chem. Res.*, 2014, **47**(8), 2631.

3 X. Y. Hu, K. Jia, Y. Cao, Y. Li, S. Qin, F. Zhou, C. Lin, D. Zhang and L. Wang, *Chem. – Eur. J.*, 2015, **21**, 1208; X. Wu, Y. Li, C. Lin, X. Y. Hu and L. Wang, *Chem. Commun.*, 2015, **51**, 6832; L. Gao, B. Zheng, W. Chen and C. A. Schalley, *Chem. Commun.*, 2015, **51**, 14901; Y. L. Sun, Y. W. Yang, D. X. Chen, G. Wang, Y. Zhou, C. Y. Wang and J. F. Stoddart, *Small*, 2013, **9**, 3224.

4 G. Sun, Z. He, M. Hao, M. Zuo, Z. Xu, X. Y. Hu, J. J. Zhu and L. Wang, *J. Mater. Chem. B*, 2019, **7**, 3944; G. Sun, Z. He, M. Hao, Z. Xu, X.-Y. Hu, J.-J. Zhu and L. Wang, *Chem. Commun.*, 2019, **55**, 10892; B. Li, Z. Meng, Q. Li, X. Huang, Z. Kang, H. Dong, J. Chen, J. Sun, Y. Dong, J. Li, X. Jia, J. L. Sessler, Q. Meng and C. Li, *Chem. Sci.*, 2017, **8**, 4458; G. Ping, Y. Wang, L. Shen, Y. Wang, X. Hu, J. Chen, B. Hu, L. Cui, Q. Meng and C. Li, *Chem. Commun.*, 2017, **53**, 7381; N. J. Wheate, K.-A. Dickson, R. R. Kim, A. Nematollahi, R. B. Macquart, V. Kayser, G. Yu, W. B. Church and D. J. Marsh, *J. Pharm. Sci.*, 2016, **105**, 3615.

5 J. Chen, H. Ni, Z. Meng, J. Wang, X. Huang, Y. Dong, C. Sun, Y. Zhang, L. Cui, J. Li, X. Jia, Q. Meng and C. Li, *Nat. Commun.*, 2019, **10**, 3546.

6 S. Kosiorek, N. Rad and V. Sashuk, *ChemCatChem*, 2020, **12**, 2776.

7 Y. Zhou, K. Jie, R. Zhao and F. Huang, *Adv. Mater.*, 2020, **32**, 1904824.

8 O. Danylyuk and V. Sashuk, *CrystEngComm*, 2015, **17**, 719.

9 A. Swartjes, P. B. White, M. Lammertink, J. A. A. W. Elemans and R. J. M. Nolte, *Angew. Chem., Int. Ed.*, 2020, **59**, 2; N. K. Beyeh, H. H. Jo, I. Kolesnichenko, F. Pan, E. Kalenius, E. V. Anslyn, R. H. A. Ras and K. Rissanen, *J. Org. Chem.*, 2017, **82**, 5198; K. Moon and E. Kaifer, *Org. Lett.*, 2004, **6**(2), 185.

10 G. Yu, X. Zhou, Z. Zhang, C. Han, Z. Mao, C. Gao and F. Huang, *J. Am. Chem. Soc.*, 2012, **134**, 19489.

11 L. D'Ascenzo and P. Auffinger, *Acta Crystallogr., Sect. B: Struct. Sci., Cryst. Eng. Mater.*, 2015, **71**, 164.

12 P. Gilli, V. Bertolasi, V. Ferretti and G. Gilli, *J. Am. Chem. Soc.*, 1994, **116**, 909; G. A. Jeffrey, *An Introduction to Hydrogen Bonding*, Oxford University Press, Oxford, 1997.

13 L. H. R. Dos Santos, B. L. Rodrigues, Y. M. Idemori and N. G. Fernandes, *J. Mol. Struct.*, 2012, **1014**, 102; L. Sobczyk, S. J. Grabowski and T. J. Krygowski, *Chem. Rev.*, 2005, **105**(10), 3513.

14 L. K. Saunders, H. Nowell, L. E. Hatcher, H. J. Shepherd, S. J. Teat, D. R. Allan, P. R. Raithby and C. C. Wilson, *CrystEngComm*, 2019, **21**, 5249; C. L. Perrin, *Acc. Chem. Res.*, 2010, **43**, 1550.

15 H. Zhang, Z. Liu, F. Xin and Y. Zhao, *Coord. Chem. Rev.*, 2020, **420**, 213425; K. Yang, K. Yang, S. Chao, J. Wen, Y. Pei and Z. Pei, *Chem. Commun.*, 2018, **54**, 9817; L.-L. Tan, H. Li, Y.-C. Qiu, D.-X. Chen, X. Wang, R.-Y. Pan, Y. Wang, S. X.-A. Zhang, B. Wang and Y.-W. Yang, *Chem. Sci.*, 2015, **6**, 1640.

16 T. R. Shattock, K. K. Arora and M. J. Zaworotko, *Cryst. Growth Des.*, 2008, **8**(12), 4533.

17 I. Ling, Y. Alias, B. W. Skelton and C. L. Raston, *Cryst. Growth Des.*, 2012, **12**, 1564.

18 R. E. Fairbairn, S. J. Teat, I. Ling and J. Dalgarno, *CrystEngComm*, 2019, **21**, 6659; P. P. Cholewa and S. J. Dalgarno, *CrystEngComm*, 2014, **16**, 3655; I. Ling, K. S. Iyer, C. S. Bond, A. N. Sobolev, Y. Aliasa and C. L. Raston, *CrystEngComm*, 2012, **14**, 8541.

19 S. Kennedy, C. M. Beavers, S. J. Teat and S. J. Dalgarno, *Cryst. Growth Des.*, 2012, **12**, 679; S. Kennedy, I. E. Dodgson, C. M. Beavers, S. J. Teat and S. J. Dalgarno, *Cryst. Growth Des.*, 2012, **12**, 688; S. Kennedy and S. J. Dalgarno, *Chem. Commun.*, 2009, 5275.

20 Y. Huang, R.-H. Gao, M. Liu, L.-X. Chen, X.-L. Ni, X. Xiao, H. Cong, Q.-J. Zhu, K. Chen and Z. Tao, *Angew. Chem., Int. Ed.*, 2020, DOI: 10.1002/anie.202002666; X.-L. Ni, X. Xiao, H. Cong, Q.-J. Zhu, S.-F. Xue and Z. Tao, *Acc. Chem. Res.*, 2014, **47**, 1386.

21 S. L. Loh, A. N. Sobolev, S. H. Lim and I. Ling, *CrystEngComm*, 2020, **22**, 52; I. Ling, H. Kumari, M. Mirzamani, A. N. Sobolev, C. J. Garvey, J. L. Atwood and C. L. Raston, *Chem. Commun.*, 2018, **54**, 10824; I. Ling, A. N. Sobolev and C. L. Raston, *CrystEngComm*, 2015, **17**, 1526.

22 L.-X. Chen, M. Liu, Y.-Q. Zhang, Q.-J. Zhu, J.-X. Liu, B.-X. Zhu and Z. Tao, *Chem. Commun.*, 2019, **55**, 14271; L. Mei, F.-Z. Li, J.-H. Lan, C.-Z. Wang, C. Xu, H. Deng, Q.-Y. Wu, K.-Q. Hu, L. Wang, Z.-F. Chai, J. Chen, J. K. Gibson and W.-Q. Shi, *Nat. Commun.*, 2019, **10**, 1532.

23 T. Ogoshi, S. Kanai, T. Yamagishi and Y. Nakamoto, *J. Am. Chem. Soc.*, 2008, **130**(15), 5022; C. Li, X. Shu, J. Li, S. Che, K. Han, M. Xu, B. Hu, Y. Yu and X. Jia, *J. Org. Chem.*, 2011, **76**(20), 8458.

24 Agilent Technologies, *CrysAlisPro, Version 1.171.38.46*.

25 G. M. Sheldrick, *Acta Crystallogr., Sect. A: Found. Adv.*, 2015, **71**, 3.

26 L. J. Farrugia, *J. Appl. Crystallogr.*, 1999, **32**, 837.

27 E. F. Pettersen, T. D. Goddard, C. C. Huang, G. S. Couch, D. M. Greenblatt, E. C. Meng and T. E. Ferrin, *J. Comput. Chem.*, 2004, **25**(13), 1605.

